

## PDF hosted at the Radboud Repository of the Radboud University Nijmegen

The following full text is a publisher's version.

For additional information about this publication click this link.

<http://hdl.handle.net/2066/205040>

Please be advised that this information was generated on 2020-09-10 and may be subject to change.



# Novel parietal epithelial cell subpopulations contribute to focal segmental glomerulosclerosis and glomerular tip lesions

see commentary on page 16

OPEN

Christoph Kuppe<sup>1</sup>, Katja Leuchtle<sup>1</sup>, Anton Wagner<sup>1</sup>, Nazanin Kabgani<sup>1</sup>, Turgay Saritas<sup>1</sup>, Victor G. Puelles<sup>1,2,3</sup>, Bart Smeets<sup>4</sup>, Samy Hakrrouch<sup>5</sup>, Johan van der Vlag<sup>6</sup>, Peter Boor<sup>1,7</sup>, Mario Schiffer<sup>8</sup>, Hermann-Josef Gröne<sup>9</sup>, Agnes Fogo<sup>10</sup>, Jürgen Floege<sup>1</sup> and Marcus Johannes Moeller<sup>1</sup>

<sup>1</sup>Division of Nephrology and Clinical Immunology, Rheinisch-Westfälische Technische Hochschule (RWTH) Aachen University, Aachen, Germany; <sup>2</sup>Cardiovascular Program, Monash Biomedicine Discovery Institute, Department of Anatomy and Developmental Biology, School of Biomedical Sciences, and Centre for Inflammatory Diseases, Monash University, Melbourne, Victoria, Australia; <sup>3</sup>Department of Nephrology, Monash Health, Melbourne Australia; <sup>4</sup>Department of Pathology, Radboud Institute for Molecular Life Sciences, Radboud Institute for Health Sciences, Radboud University Medical Center, Nijmegen, The Netherlands; <sup>5</sup>Institute of Pathology, University Medical Center, Göttingen, Germany; <sup>6</sup>Department of Nephrology, Radboud Institute for Molecular Life Sciences, Radboud Institute for Health Sciences, Radboud University Medical Center, Nijmegen, The Netherlands; <sup>7</sup>Institute of Pathology, RWTH University of Aachen, Aachen, Germany; <sup>8</sup>Department of Nephrology and Hypertension, University of Erlangen, Erlangen, Germany; <sup>9</sup>Cellular and Molecular Pathology, German Cancer Research Center, Heidelberg, Germany; and <sup>10</sup>Vanderbilt University Medical Center, Nashville, Tennessee, USA

Beside the classical flat parietal epithelial cells (PECs), we investigated proximal tubular epithelial-like cells, a neglected subgroup of PECs. These cells, termed cuboidal PECs, make up the most proximal part of the proximal tubule and may also line parts of Bowman's capsule. Additionally, a third intermediate PEC subgroup was identified at the junction between the flat and cuboidal PEC subgroups at the tubular orifice. The transgenic mouse line PEC-rtTA labeled all three PEC subgroups. Here we show that the inducible Pax8-rtTA mouse line specifically labeled only cuboidal and intermediate PECs, but not flat PECs. In aging Pax8-rtTA mice, cell fate mapping showed no evidence for significant transdifferentiation from flat PECs to cuboidal or intermediate PECs or vice versa. In murine glomerular disease models of crescentic glomerulonephritis, and focal segmental glomerulosclerosis (FSGS), intermediate PECs became more numerous. These intermediate PECs preferentially expressed activation markers CD44 and Ki-67, suggesting that this subgroup of PECs was activated more easily than the classical flat PECs. In mice with FSGS, cuboidal and intermediate PECs formed sclerotic lesions. In patients with FSGS, cells forming the tip lesions expressed markers of intermediate PECs. These novel PEC subgroups form sclerotic lesions and were more prone to cellular activation compared to the classical flat PECs in disease. Thus, colonization of Bowman's capsule by cuboidal PECs may predispose to lesion formation and chronic kidney disease.

**We propose that tip lesions originate from this novel subgroup of PECs in patients with FSGS.**

*Kidney International* (2019) **96**, 80–93; <https://doi.org/10.1016/j.kint.2019.01.037>

KEYWORDS: Columbia classification; FSGS; glomerular disease; parietal epithelial cells; tip lesions

Copyright © 2019, International Society of Nephrology. Published by Elsevier Inc. This is an open access article under the CC BY-NC-ND license (<http://creativecommons.org/licenses/by-nc-nd/4.0/>).

## Translational Statement

Here we show by genetic cell-fate tracing that glomerular epithelial lesions can be formed not only by the classical flat PECs, but also by another subgroup of PECs derived from proximal tubule-like cells. At the junction to flat PECs, proximal tubule-like cells (termed intermediate PECs) transition into a phenotype termed scattered tubular cell (STC) phenotype. In glomerular diseases such as primary FSGS, the intermediate PECs near the glomerular tuft become more numerous, proliferate sooner than classical flat PECs, and form early lesions preferentially. These findings may help to understand the pathogenesis of the different patterns of glomerular lesions, in particular the tip lesion.

Glomerular injury and subsequent FSGS account for the great majority of diseases that progress to end-stage kidney disease.<sup>1,2</sup>

**Correspondences:** Christoph Kuppe or Marcus Johannes Moeller, Department of Nephrology and Clinical Immunology, Rheinisch-Westfälische Technische Hochschule University Hospital Aachen, Pauwelsstrasse 30, 52074 Aachen, Germany. E-mail: [ckuppe@ukaachen.de](mailto:ckuppe@ukaachen.de) or [mmoeller@ukaachen.de](mailto:mmoeller@ukaachen.de)

Received 22 April 2018; revised 23 January 2019; accepted 31 January 2019; published online 27 February 2019

**W**ithin the glomerulus, classical PECs are flat cells that reside on Bowman's capsule. Recent evidence suggests that PECs are main effectors in the development of glomerulosclerotic as well as of proliferative lesions.<sup>3–7</sup>

PECs can undergo cellular activation, leading to increased capacity to proliferate, migrate, and produce extracellular

matrix. *De novo* expression of CD44 is an established marker for PEC activation,<sup>4,8,9</sup> and modulation of CD44 signaling attenuates the development of glomerulosclerotic lesions.<sup>10,11</sup> In FSGS, activated PECs and podocytes form cellular adhesions (synechia) between Bowman's capsule and the glomerular tuft.<sup>12</sup> Via this process, they are the earliest defining lesions for subsequent development of sclerotic lesions and FSGS.<sup>13–16</sup> For this reason, PEC activation has become a new potential therapeutic target in glomerular diseases.

Importantly, PEC activation is also relevant as a diagnostic tool. Markers of PEC activation have already been used in human biopsies to differentiate diseases without glomerulosclerosis, such as minimal change disease, from primary FSGS.<sup>17</sup>

Importantly for this study, PECs show a similar expression pattern as do proximal tubular cells, which have transiently acquired the STC phenotype.<sup>18</sup> The STC phenotype is a specific transcriptional program. It designates a common response pattern of proximal tubular cells to injury. Proximal tubule cells in the STC phenotype have less brush border and mitochondria particularly in humans, express specific markers *de novo* (e.g., CD44),<sup>19</sup> and proliferate more, presumably to aid tubular regeneration.<sup>18,20</sup>

In this study, we show for the first time an unexpected role of the most proximal tubular cells in the development of early FSGS lesions in animal models and patients.

## RESULTS

### PEC subgroups on Bowman's capsule

When staining for STC markers on human kidney sections (described elsewhere<sup>7,19,21</sup>), individual cells coexpressing STC markers keratin 7 and 19 (K7, K19), G protein-coupled bile acid receptor 1, and hepatocyte nuclear factor-4 were regularly observed at the tubular orifice. Remarkably, this cell was located between the classical flat PECs and the proximal tubular cells (Figure 1a–c arrowheads; Supplementary Figure S1A–C). This cell was termed intermediate PEC (iPEC).

In a minority of glomeruli, proximal tubule-like cells extended from the tubular outlet onto Bowman's capsule (Figure 1d–h, arrows). By definition, cells located on Bowman's capsule are termed PECs.<sup>22–25</sup> Thus, the proximal tubule-like cells extending onto Bowman's capsule were termed cuboidal PECs. In about one-half of the cases, cuboidal PECs were stained with lotus tetragonolobus agglutinin (LTA), indicating that they may retain their brush border in humans. In these glomeruli, the iPEC expressing STC markers was again present next to the classical flat PECs (Figure 1d–g, arrowheads). As shown in Supplementary Figure S2, glycosylated CD133 and CD24 were expressed on all flat PECs in normal human kidney. Expression was similar on all cells and there was an abrupt transition from podocalyxin-positive (podocytes) to glycosylated CD133 and CD24-positive flat PECs.

By transmission electron-microscopy, intermediate PECs were triangular in shape with a lighter cytoplasm (less ribosomes) and no brush border (Figure 1h, arrowheads).

### PEC subpopulations in mice

In healthy mice, flat PECs extended from the vascular pole along Bowman's capsule and were stained specifically for src-suppressed C-kinase (SseCKS) (Figure 1i and j, Supplementary Figure S3A).<sup>26</sup> Cuboidal PECs with a larger cytoplasm and cuboidal shape extended from the tubular pole (Figure 1i, arrows) and stained for the brush border marker LTA (Figure 1j).

Significantly more cuboidal PECs were present on Bowman's capsule in male versus female mice (Figure 1k), as reported previously.<sup>25,27</sup> On random biopsies of human tumor nephrectomies ( $n = 10$ , 40–50 glomerular cross sections each), a similar trend was noticed but did not reach significance (Figure 1g). Ultrastructurally, flat PECs were 100 to 500 nm in height (comparable to primary podocyte foot processes), with an oval-shaped nucleus (1–2  $\mu\text{m}$  in height) with condensed chromatin and an electron-lucent cytoplasm (Supplementary Figure S3B). Flat PECs had no brush border and a low number of resorption vacuoles and mitochondria. At the interface between flat and cuboidal PECs, intermediate PECs were regularly detected (Figure 1h and i, arrowheads).

In mice, STC marker cyclin D1 (CKD1) was expressed specifically in iPECs and in a graded fashion also in cuboidal PECs in normal mouse kidneys (Figure 2a and b). A schematic and summary of the marker expression profile on the PEC subgroups is shown in the next section.

### Genetic labeling of PEC subpopulations in mice

To clarify the role of PEC subpopulations *in vivo*, we found that cuboidal and iPECs could be labeled specifically in quadruple transgenic Pax8-rtTA/LC1/R26R/hist-GFP reporter mice (Figure 2c–d'''). On administration of doxycycline (dox), renal epithelial cells were labeled except for flat PECs or podocytes. Two reporter systems were used that complement each other: LC1/R26R activated cytoplasmic expression of  $\beta$ -galactosidase ( $\beta$ -Gal) irreversibly (Figure 2c). As second reporter, the nucleus was loaded with green fluorescent protein histone (hist-GFP) resulting in reversible metabolic labeling (Figure 2c). SseCKS–LTA+ cuboidal PECs and SseCKS+LTA– iPECs were marked by Pax8-rtTA mice (Figure 2d–f). SseCKS+LTA– flat PECs were not labeled, allowing us to identify and trace the new PEC subpopulations in mice. Next, the previously described quadruple-transgenic PEC-rtTA mouse was analyzed (the “parietal cell mouse”) (Figure 2g).<sup>28</sup> As shown in Figure 2h, this transgenic line labeled all 3 PEC subgroups: flat SseCKS PECs (arrows), LTA+ cPECs (arrowheads), and the iPECs in between (arrows with dots). Of note, transgenic labeling extended several cells into the proximal tubule, suggesting that these cells are different from other proximal tubular cells (Figure 2h [right angles] and i [arrows]).



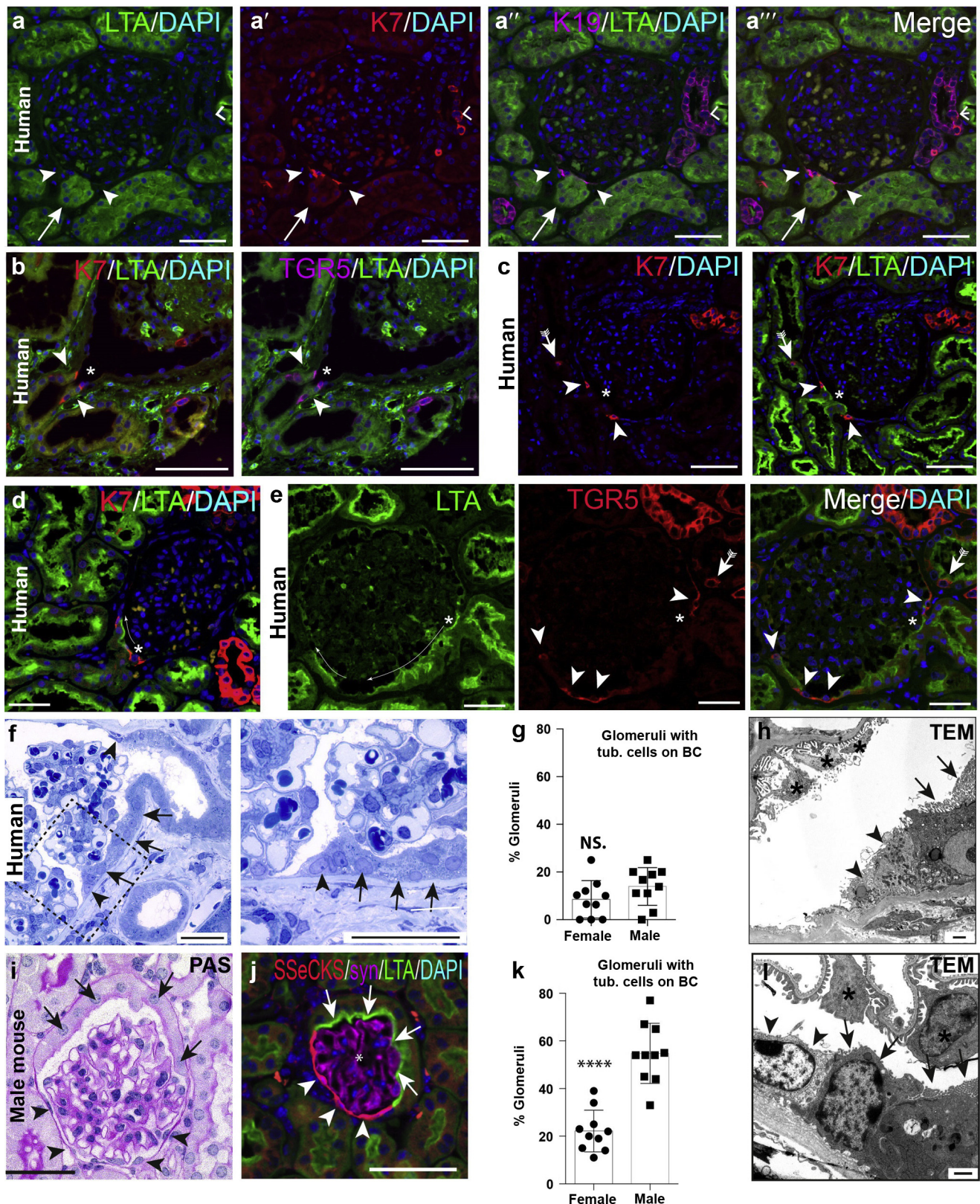


**Figure 1 | Parietal epithelial cell (PEC) subpopulations in humans and mice.** (a–e) Immunofluorescence stainings of normal human kidney shows co-expression of keratin 7 (K7), K19, and G protein–coupled bile acid receptor 1 (TGR5) in intermediate PECs at the tubular (tub.) orifice (arrowheads) and within cells of the proximal (scattered tubular cells, arrows with tails) and distal tubule (right angles). \*Podocytes (a,h). As shown in the examples (c) to (e), lotus tetragonolobus agglutinin (LTA)+ proximal tubular-like cells may extend onto Bowman’s capsule (BC; cuboidal PECs, long thin arrows). Bars = 100 μm. (f–h) Cuboidal PECs with brush border in human biopsy kidney section (arrows). In addition, (continued)



### PEC subpopulations in aging

To test whether iPECs or cuboidal PECs or both are regenerated by flat PECs or vice versa, Pax8-rtTA mice received dox at 5 weeks of age. Transgenic labeling of intermediate and cuboidal PECs was verified at 3 months of age, where virtually all LTA+ cuboidal PECs were irreversibly  $\beta$ -Gal+ (Figure 3a). In 12-month-old mice, the pattern of genetic labeling with the irreversible marker  $\beta$ -Gal was unchanged; that is, cuboidal PECs did not lose the genetic label and flat PECs did not acquire it (Figure 3a and b). These results do not support significant transdifferentiation or regeneration among the PEC subgroups in aging mice. Of note, a differential retention of the metabolic nuclear hist-GFP was observed in the aging experiments. Immediately after labeling, more than 90% of the intermediate and cuboidal PECs were labeled. Over time, hist-GFP was lost in cuboidal PECs and proximal tubule cells due to physiological turnover of the cells or only the histones in these cells. In contrast, hist-GFP was preserved in 80% and 50% of the nuclei of iPECs at 6 and 12 months of age, respectively (Figure 3c and d). To verify this finding, the same pulse chase experiment was performed using the PEC-rtTA transgenic mouse. Three months after labeling PECs, histone-eGFP was retained in 80% of iPECs, confirming our findings in Pax8-rtTA mice (Supplementary Figure S4). In contrast, histone-eGFP was lost in flat and cuboidal PECs and most other tubular cells. In summary, the unique long half-life of histones and marker expression in iPECs suggested that these cells may have distinct cellular properties.

### Differential cellular activation of PEC subpopulations

PECs become activated in FSGS, as well as in rapidly progressive glomerulonephritis.<sup>3,4</sup> *De novo* expression of activation marker CD44 was observed preferentially in iPECs within the glomeruli, which were not affected by lesions, in mice with FSGS and rapidly progressive glomerulonephritis (representative images in Figure 3e and Supplementary Figure S4C for FSGS, and Figure 3f–f' for rapidly progressive glomerulonephritis). For a statistical analysis, the Thy1.1 mouse model for FSGS was analyzed at a time point prior to lesion formation (Figure 3g–j). In this model, FSGS with prominent PEC activation can be induced by a single injection of a cytotoxic antibody to transgenic Thy1.1 expressed on podocytes.<sup>4,29,30</sup> Four days after induction, a higher percentage of cuboidal PECs expressed CD44, suggesting that these cells are more prone to activation than flat PECs (Figure 3h and i). Proliferation was highest in iPECs (90% positive),

decreasing in the neighboring cuboidal PECs, and was not increased significantly in proximal tubular epithelial cells (Figure 3j).

### Origin of cellular adhesions/synechiae in FSGS

As shown in Figure 4a, as the first defining lesion for FSGS, an adhesion is formed preferentially between flat and cuboidal PECs on Bowman's capsule and the glomerular tuft, where iPECs are localized.<sup>31</sup> To explore this further, FSGS was induced in transgenic Pax8-rtTA mice using the 5/6 nephrectomy and deoxycorticosterone acetate–salt model (Figure 4b). FSGS lesions contained enhanced green fluorescent protein (EGFP)+ intermediate or cuboidal PECs or both, suggesting that these PEC populations participate in the formation of sclerotic lesions (Figure 4c and d). The contribution of labeled PECs was higher in male versus female animals (i.e., 75% vs. 50%, respectively). Proliferative lesions (i.e., extracapillary proliferations, cellular crescents) contained almost exclusively intermediate or cuboidal PECs or both (Figure 4c, right panel). These findings were corroborated by the second irreversible reporter transgene  $\beta$ -Gal (Figure 4e).

As shown in Figure 4f and g, genetically marked PECs expressing SSeCKS became more numerous—potentially by cellular proliferation (Figure 4f, right panel). In addition, it is also possible that cuboidal PECs transitioned into the iPEC phenotype on injury or activation or both, analogous to any proximal tubular cell. As shown in Figure 4h, genetically irreversibly marked cuboidal PECs expressing  $\beta$ -Gal have lost their brush border (LTA staining) in this FSGS model, suggesting that they have transitioned at least in part into the STC phenotype to become iPECs.

Genetically marked cells can only be counted with certainty using nuclear markers, such as histone-eGFP. However, significant loss of the metabolic labeling with histone-eGFP was observed in LTA+ cuboidal PECs and proximal tubular cells in our FSGS model (Figure 4c and f, arrows with tails), which was not observed using the irreversible reporter  $\beta$ -Gal (Figure 4e). Therefore the contribution of cuboidal PECs to lesion formation was underestimated in Figure 4d using EGFP as marker in this study and may be even higher.

### Intermediate PECs as potential origin of the tip-lesion

According to the Columbia classification,<sup>32</sup> the tip variant is a unique lesion where an adhesion is formed in early FSGS close to the tubular outlet where iPECs are located and that is

**Figure 1** | (continued) intermediate PECs (arrowheads) between flat and cuboidal PECs (semithin section). Bar = 50  $\mu$ m. (g) Quantification of cuboidal PECs in tumor nephrectomies of human male and female subjects (1 dot equals mean of 40–50 glomeruli per patient,  $n = 10$  each, unpaired *t*-test; not significant [n.s.]). (h) Transmission electron microscopy (TEM) showing intermediate PECs (arrowheads) and cuboidal PECs on Bowman's capsule in human kidney. Bar = 1  $\mu$ m. (i–l) PEC subpopulations in healthy mice. (i) Periodic acid–Schiff (PAS)–staining. Bar = 50  $\mu$ m. (j) Immunofluorescent staining for src-suppressed C-kinase (SSeCKS; flat PECs, arrowheads), LTA (brush border of cuboidal PECs, arrows), and synaptopodin (\*podocytes). (k) Quantification of glomerular cross sections with LTA+ cells on Bowman's capsule (\*\*\*\* $P < 0.0001$ ,  $n = 10$  mice/sex, 25 glomerular cross sections per mouse). (l) TEM of Bowman's capsule in mice. PECs show brush border at the apical membrane (arrows with tails). Another population shows an intermediate cell phenotype with an absent brush border and reduced amount of mitochondria (arrowheads). Bar = 1000 nm. DAPI, 4',6-diamidino-2-phenylindole. To optimize viewing of this image, please see the online version of this article at [www.kidney-international.org](http://www.kidney-international.org).

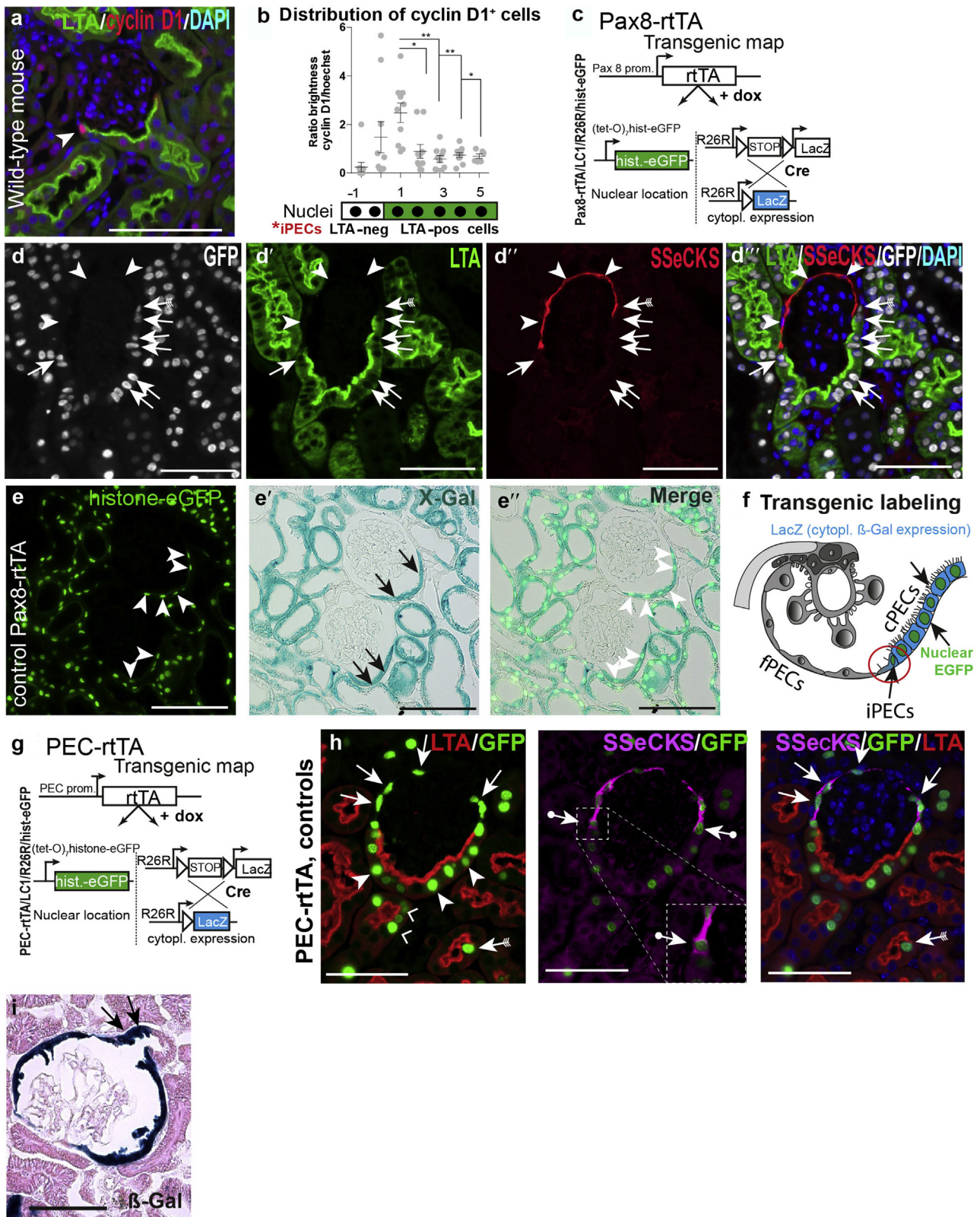


**Figure 2 | Markers for intermediate parietal epithelial cells (iPECs) in mice (a,b) and lineage tracing and immunolabeling of PEC populations (d–i).** (a) Distribution of cyclin D1<sup>+</sup> cells on Bowman’s capsule in wild-type mice. (Immunofluorescent staining for cyclin D1, red and lotus tetragonolobus agglutinin [LTA], green.) Note that cyclin D1 showed the highest expression level in presumptive iPECs between flat PECs (fPECs) and cuboidal PECs (cPECs). (b) Analysis of distribution of cyclin D1 on Bowman’s capsule (*n* = 10; shown are the mean and SDs, analysis of variance; \**P* < 0.1, \*\**P* < 0.01). (c–i) Pax8-rtTA transgenic reporter mice label cuboidal and intermediate PECs on Bowman’s capsule. (c) Transgenic map of Pax8-rtTA mice. (d) Quadruple immunofluorescent staining (continued)



prone to cellular activation. To test whether iPECs can be detected in tip lesions, human renal biopsies of early FSGS recurrences after renal transplantation showing a high frequency of tip lesions were investigated. Tip lesions were identified on periodic acid–Schiff (PAS)–stained serial sections (Figure 5a). Cells in tip lesions stained positively for the iPEC marker K7.

In a systematic analysis of 23 human biopsies diagnosed with FSGS tip lesions, FSGS lesions were visualized based on the global PEC marker annexin A3 as described previously.<sup>12</sup> Glomerulosclerotic lesions were classified into 3 groups: (i) tip variant, (ii) adhesion, that is, a synechia between the tuft and capsule away from the tubular orifice; and (iii) not otherwise specified lesion (i.e., several adhesions or advanced annexin A3+ lesions as defined in Howie *et al.*<sup>14</sup>). While 90% of tip lesions showed K7 expression, only 42% of other adhesions and 32% of not otherwise specified lesions expressed K7 (Figure 5b and c, Supplementary Figure S5). In summary, tip lesions contained the highest number of cells expressing K7 in human FSGS. This is in line with the notion that iPECs located at the tubular orifice may be the first cells to form a cellular adhesion in this situation.

## DISCUSSION

In the present study, we examined the potential relevance of 2 novel PEC subgroups (cuboidal and intermediate PECs). The cuboidal PECs at the junction to the classical flat PECs expressed STC markers, and these cells were also more prone to cellular activation and proliferation similar to proximal tubule cells, which have transitioned into the STC phenotype after injury (Figure 6). The results suggest that the epithelial interface between flat PECs and cuboidal PECs on Bowman's capsule represents a potential hot spot for FSGS lesion formation.

Our first major finding is that we have identified specific markers (see Figure 7 for a summary of the markers) and transgenic mouse lines that allow us to differentiate 3 PEC subgroups. Previously, cuboidal PECs have been reported based on their morphology in mice, rats, humans, dogs, cats, and cows.<sup>27,33–35</sup> Cuboidal PECs express markers of proximal tubular cells (e.g., the transporters Slc5a2 and Slc7a13); however, their morphology and transcriptome is not identical to those of proximal tubule cells.<sup>22,36</sup> In a single-cell transcriptomic analysis, this subgroup clustered into a distinct group of PECs rather than proximal tubule cells.<sup>37</sup> This is

supported by our observation that the PEC-specific transgenic mouse line PEC-rtTA labels intermediate and cuboidal PECs, but not proximal tubule cells, consistent with the notion that these cell populations are not identical. Intermediate PECs have been reported in various mammals based on their morphology (i.e., triangular shape), absence of apical microvilli, and low number of mitochondria.<sup>22–24</sup> Sex hormones<sup>25,27</sup> and age<sup>22</sup> have been described to modify the phenotype of the parietal epithelium, otherwise little was known so far about their potential relevance.

Low-level cellular proliferation within flat PECs has been described.<sup>38</sup> Consistent with that, we found no evidence for transdifferentiation of flat PECs into cuboidal PECs or vice versa. Previous studies have proposed a potential progenitor cell population of glycosylated CD133 and CD24–positive adult parietal epithelial multipotent progenitors in humans at this site.<sup>39,40</sup> Our findings are consistent with our previous cell fate tracing experiments in adult aging mice where no significant replenishment of other epithelial cells from PECs was observed.<sup>41,42</sup>

In our second major finding, cuboidal PECs may transition into the iPEC phenotype in glomerular disease models. The markers for injured proximal tubular cells, which have transitioned into the transient STC phenotype are also expressed by the iPEC phenotype.<sup>18,19,21</sup> Compared with neighboring proximal tubule cells, which have not transitioned into the STC phenotype, STCs lose their brush border, contain fewer mitochondria, express markers of cellular activation, and proliferate earlier and more. For these reasons, the STC phenotype was interpreted as a transient regenerative response pattern of the proximal tubule after injury, which is beneficial for regeneration of the tubule.<sup>18–20</sup> Our findings indicate that the regenerative STC phenotype is activated also in cuboidal PECs, which are derived from proximal tubule cells, causing a phenotypic transition of these cells into iPECs. Intermediate PECs showed similarities with STCs, for example, similar marker expression and higher proliferation. Two iPEC markers were identified in this study, SSeCKS and cyclin D1, which have been shown to interact with each other to regulate cellular proliferation in cultured PECs.<sup>26</sup> Furthermore, SSeCKS knockout mice formed significantly more flat PECs and developed more cellular lesions in glomerular disease,<sup>26</sup> suggesting that cells in the iPEC phenotype have an altered proliferation.

**Figure 2 |** (continued) (src-suppressed C-kinase [SSeCKS], enhanced green fluorescent protein [EGFP], LTA, and 4',6-diamidino-2-phenylindole [DAPI]) in Pax8-rtTA mice shows no labeling with EGFP in fPECs (arrowheads), whereas cPECs stained positive (pos) for EGFP. Note that SSeCKS marks fPECs and iPECs are marked by both EGFP and SSeCKS (arrows with tails). Bars = 75 μm (a,d). (e) Co-staining of histone-eGFP and X-gal staining. EGFP (arrowheads) staining was only positive in β-Gal+ cPECs (arrows). Bars = 100 μm. (f) Schematic of the labeling pattern in Pax8-rtTA quadruple transgenic mice. (g) Transgenic map of the PEC-rtTA mouse. (h) It labels SSeCKS+ fPECs (arrows), iPECs (arrows with circles), and LTA+ cPECs (arrowheads) including the proximal part of the proximal tubule (right angles). Intermediate PECs are highlighted in the inset; note that SSeCKS staining is on both sides of the green nucleus (arrows). As described previously, proximal tubular cells in the scattered tubular cell phenotype (LTA-negative) are labeled by the PEC-rtTA mouse as well (arrow with tails). Bars = 50 μm. (i) Labeling of the proximal part of the proximal tubule by the PEC-rtTA mouse visualized by the irreversible reporter β-galactosidase (β-Gal) (arrows). Bar = 50 μm. cytopl, cytoplasmic; dox, doxycycline; neg, negative; prom, promoter. To optimize viewing of this image, please see the online version of this article at [www.kidney-international.org](http://www.kidney-international.org).



Pax8-rtTA mice chased until age of 12 mo

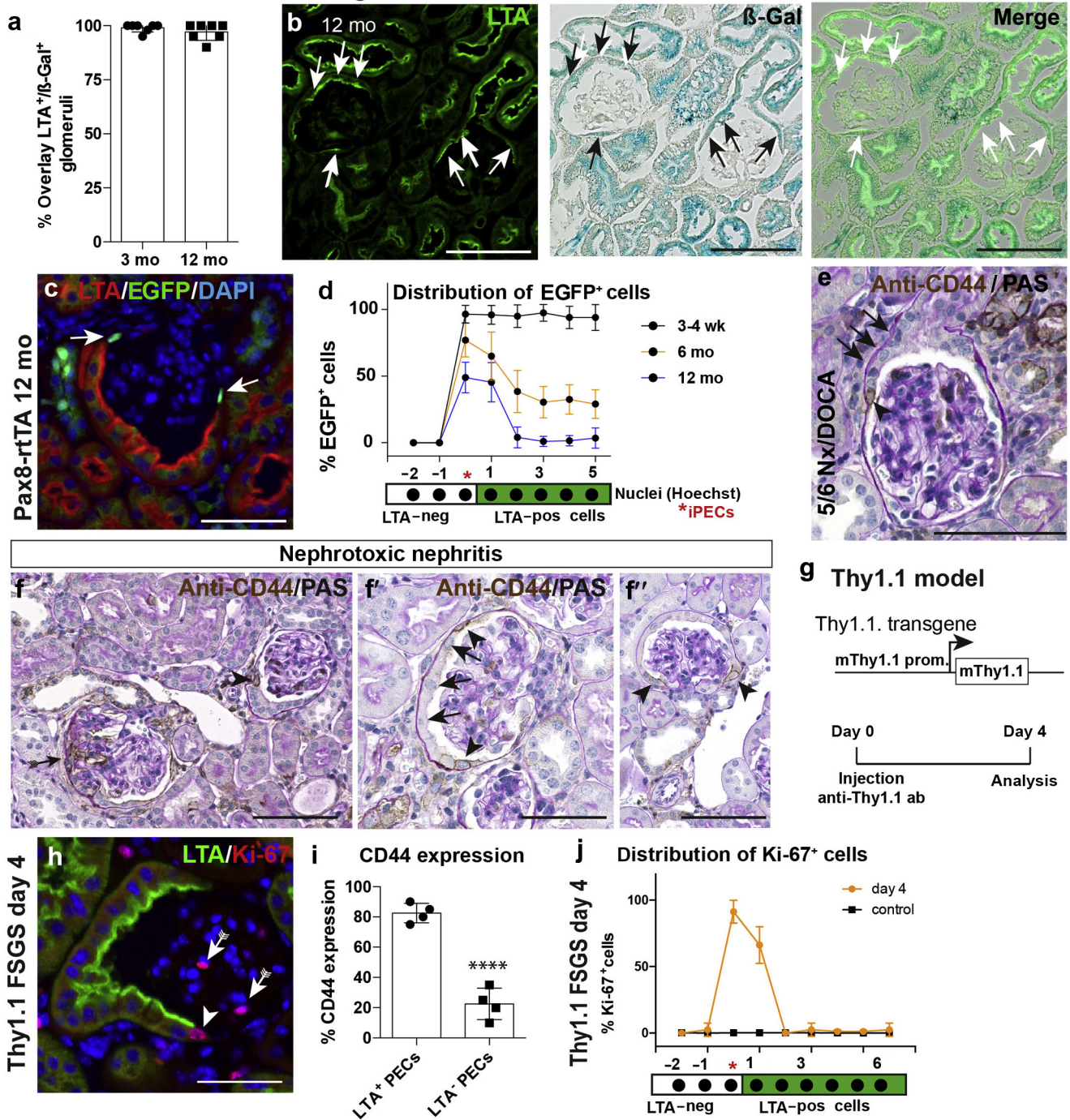


**Figure 3 | Lineage tracing of Pax8-rtTA mice (a–d) and preferential activation of intermediate parietal epithelial cells (iPECs) and cuboidal PECs (e–j).** (a) Lotus tetragonolobus agglutinin (LTA)+ PECs were nearly always positive (pos) for β-galactosidase (β-gal) at 3 months of age. (b) Co-staining of β-gal and LTA in PAX8-rtTA mice at 12 months of age shows co-expression of both markers (arrows). Bars = 100 μm. (c,d) Analysis of enhanced green fluorescent protein (EGFP) in kidneys of aged Pax8-rtTA mice. PECs located between flat PECs and cuboidal PECs showed preferentially a positive staining for EGFP (arrows). Bar = 50 μm. (d) Analysis of distribution of EGFP signal on Bowman’s capsule. n = 5 per time point. (e) CD44 immunostaining of kidneys of mice subjected to 5/6 nephrectomy (Nx) + deoxycorticosterone acetate (DOCA)-salt treatment as outlined in Figure 4b and (f) of mice treated with nephrotoxic nephritis serum to induce crescentic glomerulonephritis for 8 days. In sporadic glomeruli without lesions, CD44 was positive on Bowman’s capsule in a subset of iPECs (arrowheads) preferentially at the interface between flat PECs and cuboidal PECs (arrows in f,h). Bars = 100 μm (e,f) and 50 μm (f,f’). (g) Schematic summary of the Thy1.1 focal segmental glomerulosclerosis (FSGS) mouse model, which expresses the Thy1.1 antigen in podocytes. Acute podocyte injury and FSGS can be induced after injection of Thy1 antibody (ab) 19XE5. (h) Exemplary immunofluorescence staining of Ki-67 and LTA 4 days after induction of FSGS demonstrates preferential expression of proliferation marker Ki-67 in iPECs (arrowhead). Bar = 50 μm. (i) Analysis of *de novo* expression of CD44 in LTA-negative (neg) versus LTA+ PECs (i.e., flat vs. cuboidal PECs, respectively) in Thy1.1 mice (n = 4; 50 glomerular cross (continued)

The third major finding of this study was that proximal tubule cells (i.e., intermediate and cuboidal PECs) participate in glomerular lesion formation. Beside flat PECs and podocytes, this adds an unexpected third epithelial cell type, which may form glomerular sclerotic lesions. We found that the novel subgroup of PECs is activated sooner and proliferates more than the classical flat PECs in glomerular disease. It should be noted that flat PECs participate in lesion formation as well. Our preliminary results suggest that flat PECs form lesions somewhat later if the initiating glomerular diseases persist.

The cellular mechanism for the unusual retention of histones in iPECs in normal mice remains unclear. It could suggest a lower cellular turnover or more likely a lower turnover of the histones within the nuclei of iPECs. In any case, the finding indicates that the iPEC phenotype is stable over a longer period of time. Some kind of persistent stress or force might be the reason for the STC phenotype in the cell at the junction between flat and larger cuboidal PECs. In other tissues, interfaces between different epithelia show increased susceptibility to pathology, such as interfaces between squamous and cuboidal epithelia, such as the esophagogastric junction, or at the transformation zone of the cervix.

Fourth, we found that cuboidal PECs may extend from the proximal tubule onto Bowman's capsule also in human patients. In glomerular disease models in male experimental mice, the Bowman's capsule is colonized by cuboidal PECs, and we show data indicating that these cells transitioned into iPECs and were activated preferentially and participated in the formation of lesions. A higher prevalence of cuboidal PECs in elderly and male patients has been described,<sup>43,44</sup> and these groups of patients also have a higher risk for chronic kidney disease. In mice, virtually all FSGS models show significantly more FSGS lesions in male than in female animals. The results of this study suggest that this novel aspect of the microanatomy of the glomerulus could be associated with the individual risk of a patient to develop FSGS lesions and progression to CKD.

Finally, the results of this study suggest the epithelial interface as potential origin for lesion formation, particularly of the tip lesion at the tubular orifice.<sup>13</sup> Previous studies showed that mechanical stress or certain disease conditions cause prolapse of visceral epithelial cells (podocytes) into the proximal tubule to initiate formation of an adhesion (i.e., the tip lesion).<sup>45,46</sup> This is in line with our observations that podocytes are part of early sclerotic lesions.<sup>12,47</sup> In the present study, we show that more than 90% of the cells within tip lesions expressed iPEC markers, suggesting that iPECs (which are derived from proximal tubule cells) contribute significantly to formation of this early lesion in human patients.

The major limitation of this study is that our findings in mice using lineage tracing to identify the origin of cells cannot be translated directly to human patients for obvious technical reasons. Furthermore, we have not yet succeeded to identify a marker that labels iPECs in humans as well as in mice. Another limitation of this study is that no more than 3 markers can be stained simultaneously, so that it cannot be excluded that some cells are misclassified or go even undetected. We have tried to reduce sampling bias and artifacts due to tissue orientation as much as possible by analyzing sufficient quantities of glomeruli. Nevertheless, we do believe that the sum of the findings provides sufficient evidence to test our hypothesis further that similar pathways are relevant in human patients.

In summary, we describe the unexpected role of 2 novel PEC subgroups, which can be activated more easily than classical flat PECs and which participate in formation of glomerular lesions. Our findings support the notion that the epithelial interface between flat and cuboidal PECs is an unexpected novel hot spot of cellular activation and potential origin of lesion formation, such as the tip lesion.

## METHODS

### Experimental animals

PEC-rtTA, Pax8-rtTA, LC1, R26R, and histone-eGFP transgenic lines were on a FVB/N and Thy1.1 transgenic mice were on C57BL/6J genetic background and housed under standard specific pathogen-free conditions.<sup>3,48</sup> Most tissues from experimental animals were used from previous studies as referenced. Animal procedures were approved by the German Federal Authorities Landesamt für Natur, Umwelt, und Verbraucherschutz (LANUV) Nordrhein-Westfalen or as referenced in the text.

### Doxycycline treatment

To activate transgene expression, animals received dox via the drinking water *ad libidum* for a total of 7 or 14 days (1 mg/ml, 3% sucrose, protected from light), which was exchanged every 2 days. Subsequently, mice received tap water *ad libidum* for at least 10 days (washout period).

### Cell fate tracing and FSGS 5/6 nephrectomy–deoxycorticosterone acetate–salt model in Pax8-rtTA mice

Eight-week-old quadruple transgenic PAX8-rtTA mice received dox to induce labeling of intermediate and cuboidal PECs. For aging experiments, the kidneys were analyzed after 3, 6, and 12 months. For 5/6 nephrectomy, the mice were anesthetized deeply with ketamine-xylazine (100 mg/ml ketanest and 20 mg/ml xylazine in normal saline 0.9%; 0.1 ml/10 g of body weight) and a laparotomy was made. The vasculature of the right kidney was removed and used to verify the efficiency of the cellular labeling ( $t = 0$ ). The upper and lower poles of the left kidney were excised and Gelastyp (Sanofi-Aventis, Frankfurt, Germany) was used to stop bleeding. After 7 days, a 50-mg pellet (released over 21 days) of deoxycorticosterone acetate (DOCA; Innovative Research, Novi, MI) was implanted subcutaneously and 0.5% to 0.9% of NaCl was added to the drinking water.

Figure 3 | (continued) sections per mouse, unpaired *t*-test; \*\*\*\**P* < 0.0001). (j) Analysis of the distribution of Ki-67 expression in PECs on Bowman's capsule in Thy1.1 mice 4 days after induction. PAS, periodic acid–Schiff; prom, promoter. To optimize viewing of this image, please see the online version of this article at [www.kidney-international.org](http://www.kidney-international.org).



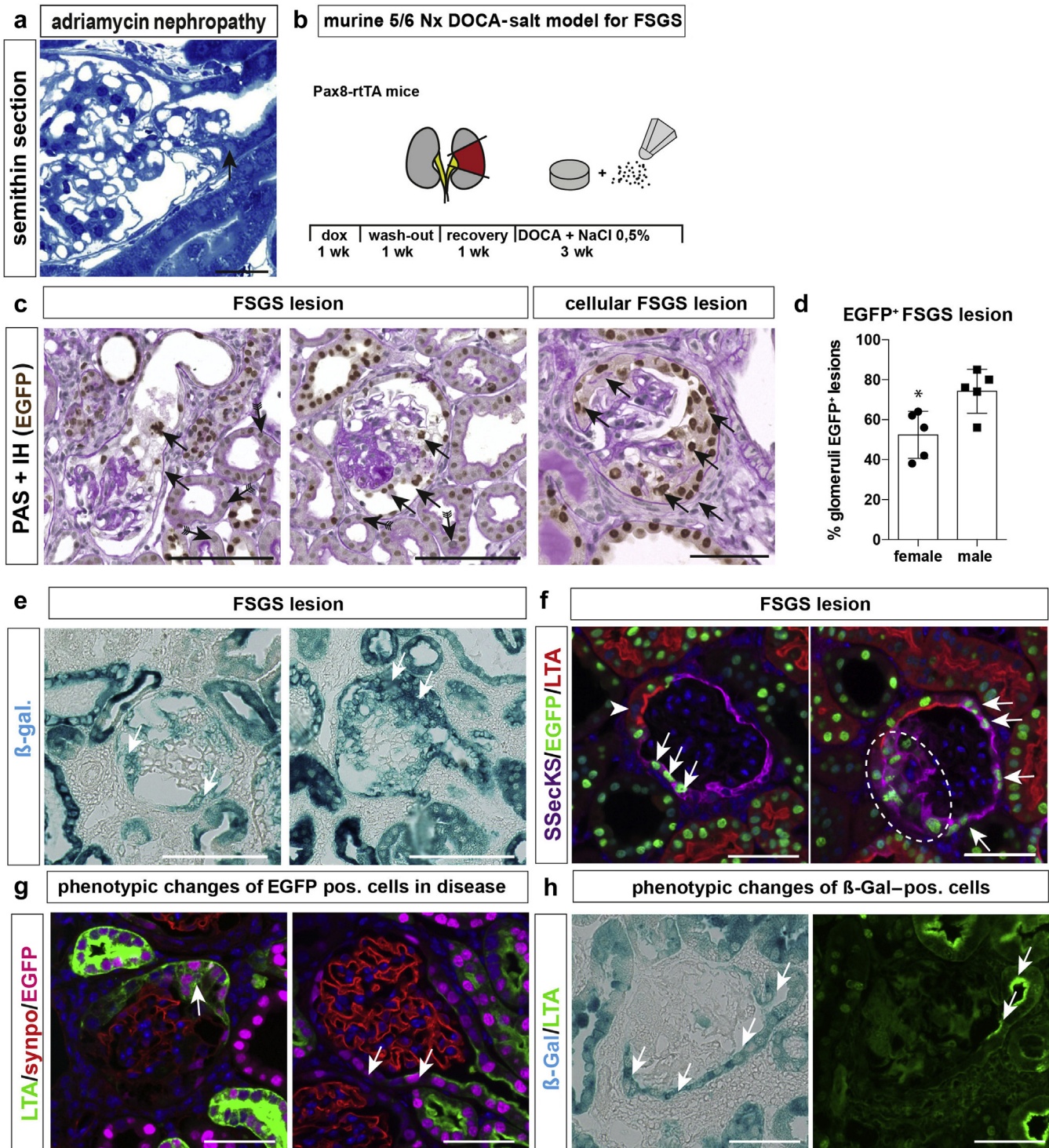


**Figure 4 | Tubularized parietal epithelial cells (PECs) contribute to focal segmental glomerulosclerosis (FSGS) lesions in mice.** (a) FSGS tip lesion (arrow) in mice treated with adriamycin to induce FSGS (arrow, semithin sections, 2 weeks after injection<sup>31</sup>). Bar = 20 μm. (b) Schematic of 5/6 nephrectomy (Nx) + deoxycorticosterone acetate (DOCA)-salt model. (c) Exemplary images of FSGS lesions show green fluorescent protein (GFP)+ cells within sclerotic lesions (arrows). Histone-eGFP is lost in some of the proximal tubular cells (arrows with tails; periodic acid-Schiff [PAS]-stainings and enhanced GFP (eGFP) immunostaining in Pax8rtTA mice). (d) Quantification of eGFP+ (pos) FSGS lesion (\*P = 0.0165, n = 5). (e) β-galactosidase (β-gal) staining of kidneys from Pax8-rtTA mice in the 5/6 nephrectomy and DOCA-salt FSGS model. (f) Presumptive FSGS lesions in the early stage (left panel) or late stage (right panel); dashed circle marks sclerotic lesion; eGFP+ cells express src-suppressed C-kinase (SSeCKS) *de novo* (arrows; cuboidal PECs, arrowhead). (g) Immunofluorescence of lotus tetragonolobus agglutinin (LTA) (green), eGFP (magenta), and synaptopodin (synpo; red) shows loss of polarized expression of LTA in eGFP+ PECs within a proliferative lesion (left) and complete loss of expression in eGFP+ cells on Bowman’s capsule (right panel). (h) Co-staining of β-gal and LTA. LTA-negative β-gal+ PECs can be observed (arrows), indicating that cuboidal PECs have lost their brush border in FSGS. Bars = 50 μm. dox, doxycycline; IH, immunohistochemistry. To optimize viewing of this image, please see the online version of this article at [www.kidney-international.org](http://www.kidney-international.org).



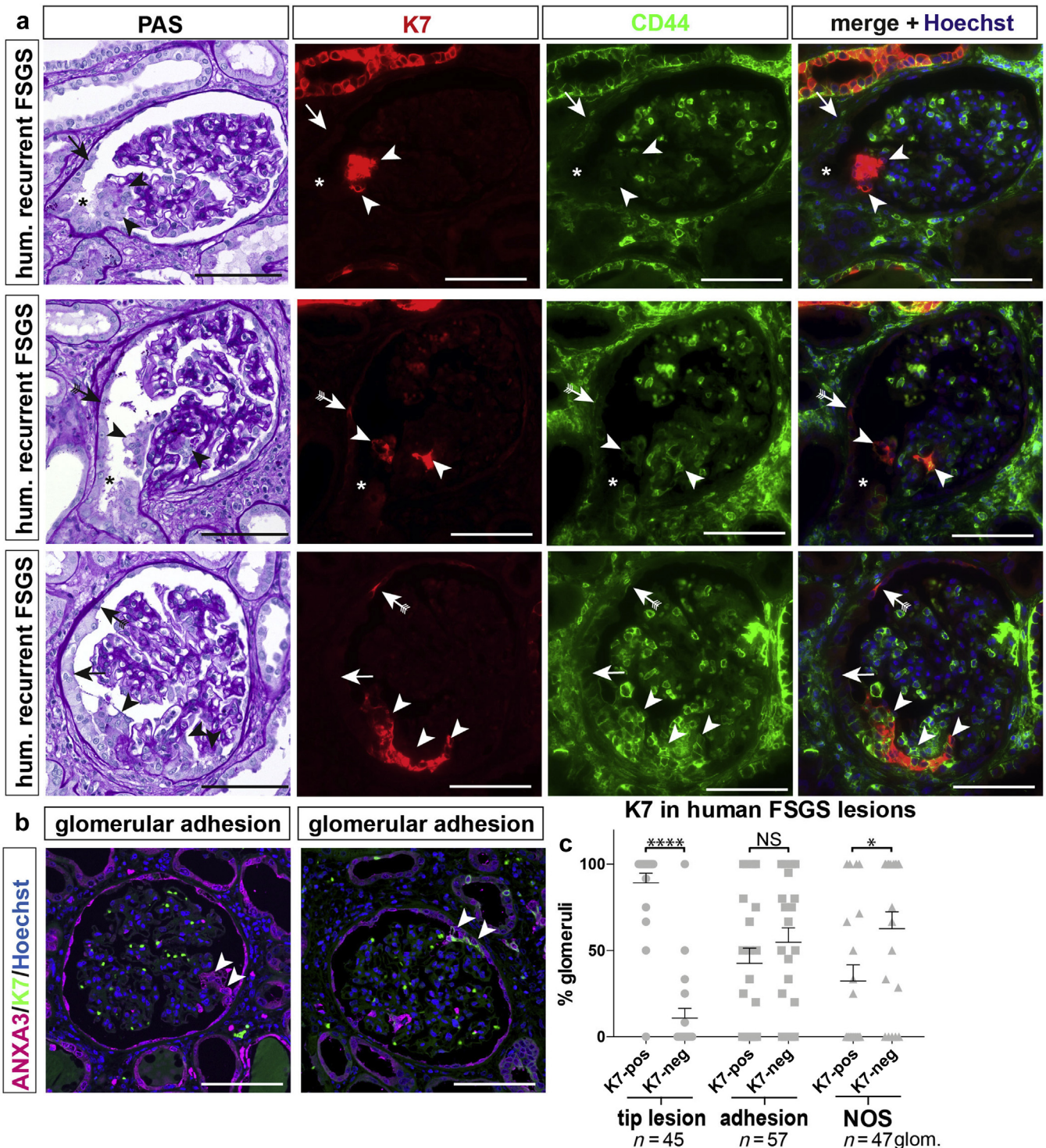


**Figure 5 | Tip lesions contain keratin 7 (K7) + (pos) cells.** Analysis of human (hum) glomerular (glom) tip lesions, adhesions, or not otherwise specified (NOS) sclerotic lesions in transplant patients with early recurrence of focal segmental glomerulosclerosis (FSGS). **(a)** Serial sections stained with periodic acid–Schiff (PAS) or immunofluorescent anti-K7 (red) and anti-CD44 (green). Cells within tip lesions were K7+ (arrowheads) but not always CD44+. K7+ cells were observed also on Bowman’s capsule (presumptive iPECs, arrows with tails). CD44 was expressed by tubular cells in the scattered tubular cell phenotype and inflammatory cells. Additional autofluorescent staining comes from erythrocytes within the glomerular tuft (green). Asterisks indicate the tubular outlet. **(b,c)** Frequency of K7+ lesions in FSGS. Exemplary images of a K7-negative (neg) (left panel) or pos (right panel) glomerular adhesion (arrowheads), visualized by the global PEC marker annexin A3 (ANXA3). **(c)** ANXA3+ tip lesions contained K7+ cells in 89.2% in 23 patients diagnosed with the tip variant of FSGS (\**P* < 0.001, \*\*\*\**P* < 0.0001, *n* = 45 glomeruli). This difference was less pronounced in other adhesions away from the tubular outlet or FSGS lesions not otherwise specified. Bar = 100 μm. NS, not significant. To optimize viewing of this image, please see the online version of this article at [www.kidney-international.org](http://www.kidney-international.org).

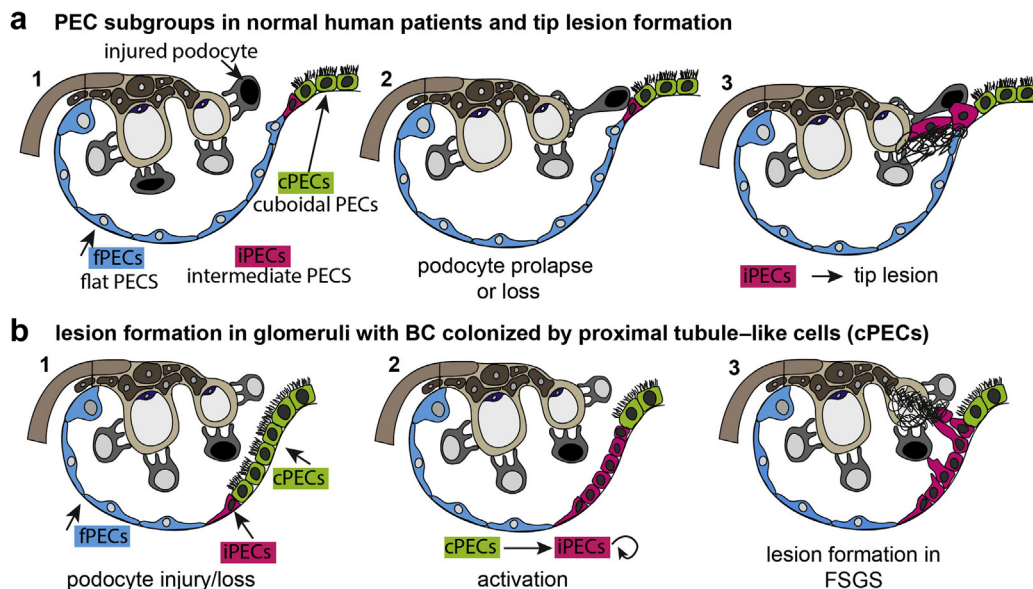


**Figure 6 | Schematic summary and proposed pathways of early lesion formation.** (a) Parietal epithelial cell (PEC) subgroups are highlighted in color. Upon glomerular injury, podocytes are injured and partially lost. Some prolapse toward the tubular outlet (black nucleus) and come into contact with intermediate PECs (iPECs) at the epithelial interface. iPECs migrate onto the glomerular tuft and deposit their matrix (tip lesion). (b) In male mice and in some human patients, proximal tubule cells extend onto Bowman's capsule (BC) and are known as cuboidal PECs (cPECs). In glomerular disease, cellular activation results in proliferation of iPECs. In addition, cPECs may transition into the intermediate phenotype. iPECs form adhesions that are not immediately at the tubular orifice. As demonstrated previously, flat PECs (fPECs) may also become activated and may proliferate and participate in lesion formation (not shown in this schematic). FSGS, focal segmental glomerulosclerosis.

During this period, general well-being, body weight, and proteinuria were closely monitored. The remnant left kidney was recovered and processed for histology. To analyze nephrotoxic nephritis, mice were analyzed 8 days after injection of anti-glomerular basement membrane serum (see Smeets *et al.*<sup>4</sup>).

**Antibody-mediated (“accelerated”) Thy-1.1 model**

Injection of anti-Thy-1.1 antibodies accelerates the development of proteinuria and FSGS in Thy-1.1 transgenic mice, resulting in an acute and massive proteinuria and dose-dependent development of collapsing FSGS lesions within 7 days. Thy-1.1 mice received an i.v. injection with 1 mg of anti-Thy-1.1 monoclonal antibody (19XE5 [clone 19XE5]) in 0.1 ml of 0.9% saline solution. Kidney samples were collected 5 days after the injection (*n* = 4).

**Perfusion fixation**

Mice were anesthetized (ketamine-rompun). The kidney(s) were perfused via the left heart ventricle with 3% paraformaldehyde in phosphate-buffered saline (pH 7.6) for 3 minutes. Pieces of the kidney(s) were snap-frozen in liquid nitrogen or (post-)fixed in 3% buffered formalin and embedded in paraffin.

**Light microscopy**

For light microscopy, the 4% buffered formalin-fixed kidney fragment were dehydrated and embedded in paraffin. Four-micrometer paraffin sections were stained with PAS. To obtain the percentage of glomeruli-containing lesions, at least 50 glomeruli per mouse were evaluated for the presence of hypertrophy and hyperplasia of the glomerular epithelium, adhesions, sclerosis, or hyalinosis.  $\beta$ -Gal

activity was detected using enzymatic  $\beta$ -galactosidase staining as described elsewhere.<sup>3</sup>

**Immunofluorescence.** Immunofluorescence staining was performed on 2- $\mu$ m paraffin-embedded sections. CD44 (R&D Systems, Minneapolis, MN), synaptopodin (P-19; Santa Cruz Biotechnology, Dallas, TX), cyclin-D1 (ab16663; Abcam, Cambridge, UK), Ki-67 (ab16667-500; Abcam), SSeCKS (homemade by Dr. Gelman), K19 (ab15463; Abcam), K7 (ab9021; Abcam), and EGFP (ab13970; Abcam) immunostaining were performed as described previously.<sup>12</sup> The following secondary antibodies were used: donkey anti-rabbit, mouse, chicken, or rat Alexa Fluor 488, Alexa Fluor 549, or Alexa Fluor 647 (Dianova, Hamburg, Germany). The nuclei were stained using Hoechst 33342 (Sigma-Aldrich, St. Louis, MO). Sections were evaluated with a Keyence BZ-9000 Microscope using BZ-II Analyzing software (Keyence Corporation, Osaka, Japan). Analysis of distributions of EGFP, cyclin-D1, and Ki-67 on Bowman's capsule was performed on sections counterstained with Hoechst and Fluorescein-labeled Lotus Tetragonolobus Lectin (LTL-FITC; Vector Laboratories, Burlingame, CA). At least in 25 glomeruli per kidney section, the location in relation to LTL-FITC of EGFP/cyclin-D1/Ki-67 was analyzed.

**Immunohistochemistry.** Immunohistochemistry was performed on 4- $\mu$ m paraffin-embedded or 3% paraformaldehyde-fixed cryosections. CD44 immunostaining were combined with a PAS staining. Sections were blocked with Avidin/Biotin Blocking Kit (Vector Laboratories) and 3% H<sub>2</sub>O<sub>2</sub>. The sections were subjected to microwave antigen retrieval in Antigen Unmasking Solution (Vector Laboratories) followed by incubation with the primary (anti-CD44) and secondary antibodies. As secondary antibodies, we used biotinylated goat anti-rat (Vector Laboratories). Detection was carried



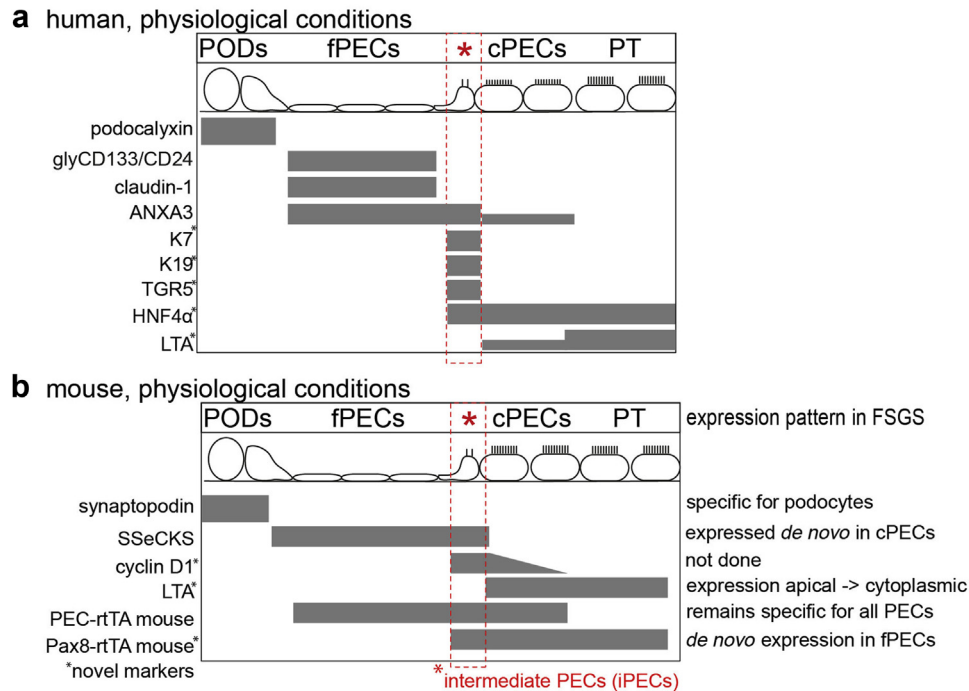


**Figure 7 | Summary of markers of this study.** Markers employed in this study to identify specific subgroups of cells within the human (a) or murine (b) glomerulus under physiological conditions. Novel markers are marked with an asterisk; the expression pattern of the markers is noted in mice in experimental focal segmental glomerulosclerosis (FSGS). ANXA3, annexin A3; cPECs, cuboidal PECs; fPECs, focal PECs; glyCD133/CD24, glycosylated CD133 and CD24; HNF4 $\alpha$ , hepatocyte nuclear factor-4; iPECs, intermediate PECs; K7, keratin 7; LTA, lotus tetragonolobus agglutinin; PEC, parietal epithelial cell; PODs, podocytes; PT, proximal tubule; SSeCKs, src-suppressed C-kinase; TGR5, G protein-coupled bile acid receptor 1.

out with Vectastain ABC kit (Vector Laboratories) with the use of peroxidase as label and 3,3-diaminobenzidine as substrate and nickel chloride enhancement. Subsequent to the immunostaining, a PAS staining was performed.

### Electron microscopy

Small pieces of renal cortex were fixed in Karnovsky's fixative, postfixed in 1% osmium tetroxide, dehydrated in ethanol and propylene oxide, and embedded in Epon resin (Serva, Heidelberg, Germany). Ultrathin sections were counterstained with 0.5% uranyl acetate and 1% lead citrate (both EMS, Munich, Germany) and examined with a Zeiss Leo 906 transmission electron microscope (Carl Zeiss, Oberkochen, Germany) at 60 kV as described previously.<sup>49</sup>

### Studies involving human kidney tissue or biopsies

The collection of human samples was approved by the local ethics committee of the Medical Faculty in Nijmegen, The Netherlands (2018-4086), the Vanderbilt University Medical Center, Nashville, Tennessee, and Aachen University (EK 221/16). Formalin-fixed paraffin-embedded sections of renal biopsies from 23 subjects with FSGS classified as tip variant according to the Columbia classification were included (Supplementary Table S1). In addition, unaffected renal tissue from patients with renal carcinoma, provided by the Eschweiler-Aachen Biobank (Germany), were used as control tissues. For analysis of cuboidal PECs in humans. Normal renal tissue from 10 male and female patients with renal carcinoma, provided by the Eschweiler-Aachen Biobank, were used for analysis (Supplementary

Table S2). All sections were evaluated with a Keyence BZ-9000 Microscope using BZ-II Analyzing software (Keyence Corporation).

### Statistics

All values are expressed as means  $\pm$  SD. For comparison of 2 groups, *t*-test was used. Comparison of several groups was performed using analysis of variance; *post hoc* Bonferroni correction was used for multiple comparisons. All tests were 2-tailed and statistical significance was defined as  $P < 0.05$ .

### DISCLOSURE

All the authors declared no competing interests.

### ACKNOWLEDGMENTS

This study was supported by the German Ministry for Science and Education (BMBF) and the German Research Foundation (DFG).

We thank Dr. Irwin Gelman for providing anti-SSeCKs antibody. This work was supported by the consortium STOP-FSGS of the German Ministry for Science and Education (BMBF 01GM1518A, to MS, PB, and MJM), and TP17, TP25, Q2 SFB/Transregio 57 and SFB/TRR219 of the DFG (to PB, JF, and MJM). CK and TS were supported by a START grant and by a Rotationsstellen program of the Faculty of Medicine of the RWTH Aachen University and by a grant of the Else-Kröner-Fresenius Foundation (A200/2013 to CK and 2015/A197 to TS). VGP is supported by the National Health and Medical Research Council of Australia (CJ Martin Research Fellowship 1128582), the Humboldt Foundation (Research Fellowship), and a research stipend by the German Society for Nephrology. BS is supported by the Netherlands Organization for Scientific Research (NWO VID):



016.156.363). Additional support came from the Interdisciplinary Center for Clinical Research Aachen within the Faculty of Medicine of RWTH Aachen University. MJM, PB, and JF are members of the SFB/Transregio 57 DFG consortium "Mechanisms of organ fibrosis." PB and MJM are Heisenberg fellows of the DFG (DFG BO3755/6-1 and MO 1082/7-1).

**SUPPLEMENTARY MATERIAL**

**Figure S1.** Scattered tubular cell markers and parietal epithelial subpopulations. Immunofluorescent staining for keratin 7 (K7), K19, hepatocyte nuclear factor-4 (HNF4 $\alpha$ ) and lotus tetragonolobus agglutinin (LTA). **(A)** HNF4 $\alpha$  marks proximal tubular cells (inset). Note that K7+ cells were located in conjunction to HNF4 $\alpha$  at the tubular-glomerular junction. **(B)** HNF4 $\alpha$ + cells could be detected on Bowman's capsule. Note that K7+ cells were located in conjunction to HNF4 $\alpha$ + cells. **(C)** K19+ cells can be detected in direct conjunction to LTA+ tubular cells (arrow). Bars = 100  $\mu$ m.

**Figure S2.** Analysis of CD24/glycosylated CD133 (glyCD133) on Bowman's capsule. **(A,B)** Schematic of the nomenclature. **(B)** According to previous reports, a graded expression of progenitor markers into podocyte markers (PDX) indicated continuous podocyte regeneration. **(C,D)** Representative immunofluorescent co-stainings of podocalyxin (podocytes), claudin-1 (fPECs), and either CD24 or glyCD133. Bar = 100  $\mu$ m. **(E)** Expression of glyCD133 and claudin-1 as percentage of the circumference of Bowman's capsule in normal human kidney (total of 238 glomeruli in 6 different nephrectomy specimens). PODs, podocytes; CD133+CD24+PDX-PECs, presumptive localization of renal progenitors (red circle), cPEC; cuboidal PEC; fPEC, focal PEC; PDX, podocalyxin; PEC, parietal epithelial cell.

**Figure S3.** Parietal epithelial cell (PEC) subpopulations in mice and humans. **(A)** Immunofluorescent staining for src-suppressed C-kinase (S $\text{SeCKS}$ , which are focal PECs), lotus tetragonolobus agglutinin (LTA, which are cuboidal PECs), and synaptopodin (podocytes). **(B)** Electron microscopy (EM) overview of Bowman's capsule in mice. Inset marks image selection for Figure 11. Cuboidal PECs form a brush border at the apical membrane (arrows). Focal PECs are marked with arrowheads. **(C)** Normal human kidney section from tumor nephrectomies stained with LTA (cuboidal PECs). Note that 3 glomeruli show LTA+ cells on Bowman's capsule (arrows) close to the tubular pole (arrows with tails). Glomeruli are marked by asterisks. Bars = 100  $\mu$ m.

**Figure S4.** **(A)** In the PEC-rtTA mouse after a pulse chase period of 3 months, the histone-eGFP metabolic label persisted preferentially in intermediate parietal epithelial cells (iPECs) (arrows). **(B)** Analysis of enhanced green fluorescent protein (EGFP)+ nuclei on Bowman's capsule in aged PEC-rtTA mice ( $n = 5$ , analysis of variance,  $P < 0.001$ ). **(C)** In Pax8-rtTA mice subjected to 5/6 nephrectomy and deoxycorticosterone acetate (DOCA)-salt treatment to induce focal segmental glomerulosclerosis (FSGS) lesions, CD44 was expressed in the EGFP+ presumptive iPECs (arrowhead). In the example shown, the adjacent cuboidal PEC has also retained its GFP-histone labeling but does not express activation marker CD44 (arrow). Labeling within tubular cells is marked by arrows with tails. Bars = 50  $\mu$ m. LTA, lotus tetragonolobus agglutinin.

**Figure S5.** Keratin 7 (K7)+ cells (presumptive intermediate parietal epithelial cells) within focal segmental glomerulosclerosis lesions. **(A)** Examples of a tip lesion with little K7 expression (arrowheads). **(B)** Example of a lesion not otherwise specified (NOS) containing a mixture of K7+ (arrowheads) or K7-negative (arrows) adhesions and lesions. Immunofluorescent co-stainings for the global parietal epithelial cell marker annexin A3 (ANXA3) and K7. Bars = 100  $\mu$ m.

**Table S1.** Demographics of patients classified with focal segmental glomerulosclerosis (FSGS).

**Table S2.** Demographics of patients with kidney tumor nephrectomies.

Supplementary material is linked to the online version of that paper at [www.kidney-international.org](http://www.kidney-international.org).

**REFERENCES**

1. Levey AS, Coresh J. Chronic kidney disease. *Lancet*. 2012;379:165–180.
2. Wiggins RC. The spectrum of podocytopathies: a unifying view of glomerular diseases. *Kidney Int*. 2007;71:1205–1214.
3. Smeets B, Kuppe C, Sicking EM, et al. Parietal epithelial cells participate in the formation of sclerotic lesions in focal segmental glomerulosclerosis. *J Am Soc Nephrol*. 2011;22:1262–1274.
4. Smeets B, Uhlig S, Fuss A, et al. Tracing the origin of glomerular extracapillary lesions from parietal epithelial cells. *J Am Soc Nephrol*. 2009;20:2604–2615.
5. Bollee G, Flamant M, Schordan S, et al. Epidermal growth factor receptor promotes glomerular injury and renal failure in rapidly progressive crescentic glomerulonephritis. *Nat Med*. 2011;17:1242–1250.
6. Djurdjaj S, Lue H, Rong S, et al. Macrophage migration inhibitory factor mediates proliferative GN via CD74. *J Am Soc Nephrol*. 2016;27:1650–1664.
7. Djurdjaj S, Papisotiriou M, Bulow RD, et al. Keratins are novel markers of renal epithelial cell injury. *Kidney Int*. 2016;89:792–808.
8. Fatima H, Moeller MJ, Smeets B, et al. Parietal epithelial cell activation marker in early recurrence of FSGS in the transplant. *Clin J Am Soc Nephrol*. 2012;7:1852–1858.
9. Shankland SJ, Smeets B, Pippin JW, et al. The emergence of the glomerular parietal epithelial cell. *Nat Rev Nephrol*. 2014;10:158–173.
10. Roeder SS, Barnes TJ, Lee JS, et al. Activated ERK1/2 increases CD44 in glomerular parietal epithelial cells leading to matrix expansion. *Kidney Int*. 2017;91:896–913.
11. Eymael J, Sharma S, Loeven MA, et al. CD44 is required for the pathogenesis of experimental crescentic glomerulonephritis and collapsing focal segmental glomerulosclerosis. *Kidney Int*. 2018;93:626–642.
12. Kuppe C, Grone HJ, Ostendorf T, et al. Common histological patterns in glomerular epithelial cells in secondary focal segmental glomerulosclerosis. *Kidney Int*. 2015;88:990–998.
13. Howie AJ, Brewer DB. The glomerular tip lesion: a previously undescribed type of segmental glomerular abnormality. *J Pathol*. 1984;142:205–220.
14. Howie AJ, Pankhurst T, Sarioglu S, et al. Evolution of nephrotic-associated focal segmental glomerulosclerosis and relation to the glomerular tip lesion. *Kidney Int*. 2005;67:987–1001.
15. Van Damme B, Tardanico R, Vanrenterghem Y, et al. Adhesions, focal sclerosis, protein crescents, and capsular lesions in membranous nephropathy. *J Pathol*. 1990;161:47–56.
16. Kriz W, Gretz N, Lemley KV. Progression of glomerular diseases: is the podocyte the culprit? *Kidney Int*. 1998;54:687–697.
17. Smeets B, Stucker F, Wetzels J, et al. Detection of activated parietal epithelial cells on the glomerular tuft distinguishes early focal segmental glomerulosclerosis from minimal change disease. *Am J Pathol*. 2014;184:3239–3248.
18. Berger K, Moeller MJ. Mechanisms of epithelial repair and regeneration after acute kidney injury. *Semin Nephrol*. 2014;34:394–403.
19. Smeets B, Boor P, Dijkman H, et al. Proximal tubular cells contain a phenotypically distinct, scattered cell population involved in tubular regeneration. *J Pathol*. 2013;229:645–659.
20. Berger K, Bange JM, Hammerich L, et al. Origin of regenerating tubular cells after acute kidney injury. *Proc Natl Acad Sci U S A*. 2014;111:1533–1538.
21. Lindgren D, Bostrom AK, Nilsson K, et al. Isolation and characterization of progenitor-like cells from human renal proximal tubules. *Am J Pathol*. 2011;178:828–837.
22. Haley DP, Bulger RE. The aging male rat: structure and function of the kidney. *Am J Anat*. 1983;167:1–13.
23. Lee SJ, Sparke J, Howie AJ. The mammalian glomerulotubular junction studied by scanning and transmission electron microscopy. *J Anat*. 1993;182:177–185.
24. Ojeda JL, Icardo JM. A scanning electron microscope study of the neck segment of the rabbit nephron. *Anat Embryol (Berl)*. 1991;184:605–610.
25. Crabtree C. Sex differences in the structure of Bowman's capsule in the mouse. *Science*. 1940;91:299.

26. Burnworth B, Pippin J, Karna P, et al. SSeCKS sequesters cyclin D1 in glomerular parietal epithelial cells and influences proliferative injury in the glomerulus. *Lab Invest*. 2012;92:499–510.
27. Carpino F, Barberini F, Familiari G, et al. Columnar cells of the parietal layer of Bowman's capsule and their relationship with the sexual cycle in normal female mice. *Experientia*. 1976;32:1584–1585.
28. Appel D, Kershaw DB, Smeets B, et al. Recruitment of podocytes from glomerular parietal epithelial cells. *J Am Soc Nephrol*. 2009;20:333–343.
29. Kollias G, Evans DJ, Ritter M, et al. Ectopic expression of Thy-1 in the kidneys of transgenic mice induces functional and proliferative abnormalities. *Cell*. 1987;51:21–31.
30. Smeets B, Te Loeke NA, Dijkman HB, et al. The parietal epithelial cell: a key player in the pathogenesis of focal segmental glomerulosclerosis in Thy-1.1 transgenic mice. *J Am Soc Nephrol*. 2004;15:928–939.
31. Hakrout S, Cebulla A, Schaldecker T, et al. Extensive podocyte loss triggers a rapid parietal epithelial cell response. *J Am Soc Nephrol*. 2014;25:927–938.
32. D'Agati VD, Fogo AB, Bruijn JA, et al. Pathologic classification of focal segmental glomerulosclerosis: a working proposal. *Am J Kidney Dis*. 2004;43:368–382.
33. Haensly WE, Granger HJ, Morris AC, et al. Proximal-tubule-like epithelium in Bowman's capsule in spontaneously hypertensive rats: changes with age. *Am J Pathol*. 1982;107:92–97.
34. von Möllendorff W. *Handbuch der Mikroskopischen Anatomie des Menschen*. Berlin, Germany: Springer Verlag; 1930.
35. Dietert SC. The columnar cells occurring in the parietal layer of Bowman's capsule: cellular fine structure and protein transport. *J Cell Biol*. 1967;35:435–444.
36. Cheval L, Pierrat F, Dossat C, et al. Atlas of gene expression in the mouse kidney: new features of glomerular parietal cells. *Physiol Genomics*. 2011;43:161–173.
37. Sivakamasundari V, Bolisetty M, Sivajothi S, et al. Comprehensive cell type specific transcriptomics of the human kidney. December 22, 2017. Available at: <https://www.biorxiv.org/content/10.1101/238063v1>. Accessed January 2018.
38. Pabst R, Sterzel RB. Cell renewal of glomerular cell types in normal rats: an autoradiographic analysis. *Kidney Int*. 1983;24:626–631.
39. Sagrinati C, Netti GS, Mazzinghi B, et al. Isolation and characterization of multipotent progenitor cells from the Bowman's capsule of adult human kidneys. *J Am Soc Nephrol*. 2006;17:2443–2456.
40. Lazzeri E, Crescioli C, Ronconi E, et al. Regenerative potential of embryonic renal multipotent progenitors in acute renal failure. *J Am Soc Nephrol*. 2007;18:3128–3138.
41. Berger K, Schulte K, Boor P, et al. The regenerative potential of parietal epithelial cells in adult mice. *J Am Soc Nephrol*. 2014;25:693–705.
42. Wanner N, Hartleben B, Herbach N, et al. Unraveling the role of podocyte turnover in glomerular aging and injury. *J Am Soc Nephrol*. 2014;25:707–716.
43. Hodgin JB, Bitzer M, Wickman L, et al. Glomerular aging and focal global glomerulosclerosis: a podometric perspective. *J Am Soc Nephrol*. 2015;26:3162–3178.
44. Carrero JJ, Hecking M, Chesnaye NC, Jager KJ. Sex and gender disparities in the epidemiology and outcomes of chronic kidney disease. *Nat Rev Nephrol*. 2018;14:151–164.
45. Howie AJ, Ferreira MA, Majumdar A, et al. Glomerular prolapse as precursor of one type of segmental sclerosing lesions. *J Pathol*. 2000;190:478–483.
46. Howie AJ, Lee SJ, Sparke J. Pathogenesis of segmental glomerular changes at the tubular origin, as in the glomerular tip lesion. *J Pathol*. 1995;177:191–199.
47. Giannico G, Yang H, Neilson EG, et al. Dystroglycan in the diagnosis of FSGS. *Clin J Am Soc Nephrol*. 2009;4:1747–1753.
48. Hakrout S, Moeller MJ, Theilig F, et al. Effects of increased renal tubular vascular endothelial growth factor (VEGF) on fibrosis, cyst formation, and glomerular disease. *Am J Pathol*. 2009;175:1883–1895.
49. Babickova J, Klinkhammer BM, Buhl EM, et al. Regardless of etiology, progressive renal disease causes ultrastructural and functional alterations of peritubular capillaries. *Kidney Int*. 2017;91:70–85.